Original Article
Effect of miR-96-5p targeting of the PRC1 gene on proliferation, apoptosis and invasion in hepatoma HepG2 cells

Xuebin Peng, Min Li, Aiping Tian, Ni Jiang, Yongwu Mao, Ting Li, Xiaorong Mao

Department of Infectious Diseases, The First Hospital of Lanzhou University, Lanzhou, Gansu Province, China

Abstract: Objective: This study aimed to explore the effect of miR-96-5p targeting of PRC1 (protein regulator of cytokinesis 1) gene on proliferation, apoptosis and invasion of hepatoma HepG2 cells. Methods: LO2 and HepG2 cells were cultured *in vitro* for the study. The targeted relationship between miR-96-5p and PRC1 was verified by dual-luciferase reporter gene assay. HepG2 cells were separately transfected within seven groups including; Control group, mimic NC group, miR-96-5p mimic group, miR-96-5p inhibitor group, oe NC group, oe PRC1 group, and miR-96-5p mimic + oe PRC1 group. Expression of miR-96-5p and PRC1 were detected by quantitative reverse transcriptase PCR and western blot. Proliferation activity was detected by 5-ethynyl-2'-deoxyuridine (EdU); cell cycle and apoptosis were determined by flow cytometry. Cell metastasis and invasion were assessed by Transwell assay. The effects of the overexpression of PRC1 or miR-361-5p on tumor growth were evaluated through tumorigenesis experiment in nude mice. Results: Compared with normal liver LO2 cells, miR-96-5p expression was down-regulated and PRC1 expression was up-regulated in hepatoma HepG2 cells. Dual-luciferase reporter gene assay showed that there is a targeted relationship between miR-96-5p and PRC1. miR-96-5p targeted the 3' untranslated region (3'UTR) of the PRC1 gene and down-regulated its expression. Overexpression of miR-96-5p could inhibit proliferation, migration and invasion of HepG2 cells, suppress tumor growth and promote cell apoptosis. Inversely, overexpression of PRC1 elicited an opposite response. Meanwhile, overexpression of both miR-96-5p and PRC1 in miR-96-5p mimic + oe PRC1 group, compared with miR-96-5p mimic group, presented an enhancement of proliferation, migration and invasion of HepG2 cells as well as inhibition on apoptosis. While compared with oe PRC1 group, HEPG 2 cells in miR-96-5p mimic + oe PRC1 group presented with significantly opposite effects. Conclusion: miR-96-5p targeting of PRC1 gene inhibits proliferation and invasion of hepatoma HepG2 cells and promotes their apoptosis.

Keywords: miR-96-5p, protein regulator of cytokinesis 1, HepG2, cell proliferation, apoptosis

Introduction

More than 600,000 patients worldwide die of liver cancer every year, and the half occur in China; plus, the morbidity and mortality in China rank the highest in the world [1, 2]. Liver cancer arises with relatively obscure symptoms in early stage, while it often is found and diagnosed in an advanced stage in most patients upon first consultation [3, 4]. Surgery, chemical drugs, and radiotherapy are the main choices for early treatment, but these methods have certain limitations, such as strong side effects and incomplete treatment [5]. Therefore, it is necessary to explore the pathogenesis of liver cancer based on the existing methods and find

new therapeutic targets for better effective treatment.

In recent years, with the development of molecular biotechnology, targeted therapy has presented as a hot spot in liver cancer treatment. Lots of studies have stated that microRNAs serve as a crucial regulatory role in human physiological and pathological processes by inhibiting protein translation of target genes [6, 7]. MiRNAs play a key role in the occurrence and progression of tumor and cancer, which can affect various biological behaviors like cell growth, proliferation, invasion and metastasis [8-10]. Some researchers have found that miR-150-5p presents with low expression in hepa-

toma cells, and its increased expression can restrain cell migration and invasion [11].

Protein regulator of cytokinesis 1 (PRC1), encoded by the PRC1 gene, is a potential target for developing anti-cancer drugs in cancer treatment. PRC1, was first discovered in 1998, it is located on human chromosome 15 and consists of 620 amino acids [12, 13]. PRC1 is a novel protein molecule related to cell cycle regulation, which is mainly expressed in G2/M phases and is additionally a substrate of several cyclin-dependent kinases [14]. PRC1 plays an important role in the occurrence and progression of various tumors as found in research. For example, PRC1 participates in the proliferation, invasion, and apoptosis of hepatoma cells and could be a potential oncogene [15]. We found a miR-96-5p binding site on PRC1 through bioinformatics analysis, thus, it is tempting to speculate that miR-96-5p could target PRC1 to affect the proliferation, apoptosis and invasion of hepatoma HepG2 cells.

Materials and methods

Cell culture and transfection

The human hepatocellular carcinoma cell line HepG2 and immortalized normal human hepatic cell line LO2 were purchased from the Cell Bank of Type Culture Collection of Shanghai Institute for Biological Sciences, Chinese Academy of Sciences. The cells were cultured in DMEM supplemented with 10% FBS, 100 µg/mL streptomycin, and 100 U/mL penicillin, at 37°C in an incubator with 5% CO_2. The culture medium was changed 3 or 4 times a week depending on the growth status. The cells were passaged when reaching approximately 80% confluency.

Cell transfection was performed through lentivirus vector, and the HepG2 cells were divided into seven groups: control group (blank control), mimic NC group (microRNA negative control), miR-96-5p mimic group (miR-96-5p overexpression), miR-96-5p inhibitor group (miR-96-5p inhibitor), oe NC group (PRC1 negative control), oe PRC1 group (PRC1 overexpression), and miR-96-5p mimic + oe PRC1 group (overexpression of both miR-96-5p and PRC1). The plasmids used in the study were purchased from Vigene Biosciences, Inc. (Rockville, MD, USA). The overexpressed fragment and target

pLVX-IRES-ZsGreen1 vector were digested by restriction enzymes EcoRI and BamHI, respectively, followed by ligation. The ligated products were then transformed into competent Escherichia coli DH5α cells, and the positive recombinant clones were verified by sequencing. High-purity endotoxin-free plasmids were extracted from a total of 20 µg of psPAX2 (Invitrogen, Grand Island, NY, USA) and pMD2G (Invitrogen) with recombinant plasmids, and then co-transfected into 293T cells to package the lentivirus. The culture supernatant rich in recombinant lentivirus particles from these cells for each group was collected after 48-72 h transfection, and was concentrated to obtain high-titer lentivirus solution. The supernatant with lentivirus higher than 107 TU/ml was stored at -80°C for later use. The human hepatoma HepG2 cells in logarithmic growth phase were inoculated into 6-well plates, and the culture supernatant was discarded after 24 h culture. The HepG2 cells were then infected with different lentivirus supernatants separately (MOI=20) in the presence of polybrene at a concentration of 5 µg/mL. The culture plate was gently shaken every 15 min to make sure the cells were fully in contact with the lentivirus, and after 2 h, the plate was placed in an incubator to continue culturing for 10 h. Then the virus-containing culture medium was replaced with normal culture medium for another 24 h culture. Subsequently, GFP expression was observed by fluorescence microscopy. Stably transfected HepG2 cells were seeded in 6-well plates. The culture medium was replaced with serum-free DMEM when the cell confluency reached more than 80%. After 24 h, the serum-free DMEM was replaced with DMEM supplemented with 10% FBS for further 48 h culture. Then the cells were used in subsequent experiments.

Dual-luciferase reporter gene assay

The PRC1 3'UTR sequences containing wild-type or mutant miR-96-5p binding sites were synthesized and inserted respectively into the 3'UTR of the luciferase gene in pMIR-reporter (Thermo Fisher Scientific, Waltham, MA, USA) to construct recombinant vectors, pMIR-PRC1-WT and pMIR-PRC1-MT. The luciferase reporter plasmids PRC1-WT and PRC1-MT with correct sequencing were co-transfected with miR-96-5p into HEK293T cells respectively. The renilla

Table 1. Primer sequences

Gene name	Forward primer (5'-3')	Reverse primer (5'-3')
miR-96-5p	TTTGGCACTAGCACAT	GAGCAGGCTGGAGAA
U6	ATTGGAACGATACAGAGAAGAT	GGAACGCTTCACGAATTT
PRC1	GCTGAGATTGTGCGGTTA	GCCTTCAACTCTTCTTCCA
GADPH	GAAGGTGAAGGTCGGAGTC	GAAGATGGTGATGGGATT

Note: PRC1: protein regulator of cytokinesis 1; GAPDH: glyceraldehyde 3-phosphate dehydrogenase.

luciferase was used as the internal control. The cells were collected and lysed 48 h after transfection. The luciferase activity was measured using a dual-luciferase reporter assay kit (Promega, WI, USA) according to the manufacturer's instructions. The firefly and renilla luciferases activities were sequentially measured for a single sample in a luminometer. The ratio of firefly luciferase activity to renilla luciferase activity was taken as the relative luciferase activity for statistical analysis.

Quantitative reverse transcriptase PCR

Total RNA from cells was extracted using TRIzol® reagent (Invitrogen, Carlsbad, CA, USA), and the concentration and purity of extracted total RNA were detected by Thermo Scientific™ NanoDrop™ 2000 micro-volume spectrophotometer (NanoDrop, USA). Reverse transcription was carried out on 1 µg of total RNA by using the PrimeScript™ RT Reagent Kit with gDNA Eraser (TaKaRa, Japan). Genomic DNA elimination reaction was carried out at 42°C for 2 min after adding 5×g DNA Eraser Buffer and gDNA Eraser, followed by reverse transcription reaction at 37°C for 15 min and 85°C for 5 s to obtain cDNA. Real-time polymerase chain reaction (PCR) was performed with SYBR® Premix EX Taq™ (Tli RNaseH plus) (Takara, Japan) on ABI 7500 Fast Real-Time PCR instrument (Applied Biosystems, USA). The reaction conditions were as follows: pre-denaturation at 95°C for 10 min, followed by 40 cycles of denaturation at 95°C for 15 s and annealing at 60°C for 30 s, and lastly extension at 72°C for 2 min. U6 served as an internal control for miR-96-5p, and GAPDH (glyceraldehyde 3-phosphate dehydrogenase) was used as the internal control for other genes. The fold change was calculated by the $2^{-\Delta\Delta Ct}$ method. $\Delta\Delta Ct$ = $\Delta Ct_{experimental\ group}$ - ΔCt_{gapdh}, in which ΔCt = $Ct_{target\ gene}$ - $Ct_{internal\ control}$. Here, Ct refers to the amplification cycles when the real-time fluorescence intensity reached the set threshold, and the amplification was in logarithmic growth. The primers used were shown in **Table 1**. All primers were provided by Shanghai GenePharma Co., Ltd., China.

Western blot

The concentration of the total protein extracted from cells was measured using BCA protein assay reagent kit (Thermo Fisher Scientific, Waltham, MA, USA). The total protein received polyacrylamide gel electrophoresis at a constant voltage of 80 V for 35 min and 120 V for 45 min. The proteins were then transferred to polyvinylidene fluoride (PVDF) membranes (Merck Millipore, Billerica, MA, USA). The membranes were blocked with 5% BSA for 1 h at room temperature, and then washed with PBST buffer after discarding the blocking buffer. Subsequently, the membranes were incubated with primary rabbit monoclonal antibodies against PRC1 (1:5,000; Abcam, UK) and GAPDH (1:10,000; Abcam, UK) overnight at 4°C, and then washed by PBS buffer containing 0.1% Tween-20 3 times for 10 min each time. The membranes were subsequently incubated at room temperature for 1 h after adding horseradish peroxidase labeled sheep anti-rabbit antibody (1:10,000; Jackson, USA), followed by washing with PBST buffer 3 times for 10 min each time. After incubation, the membranes were immersed in the enhanced chemiluminescence (ECL) reaction solution (Pierce Company, USA) at room temperature for 1 min. After being removed out of the reaction solution, the membranes were covered with preservative film, and exposed to an X-ray film in the dark, followed by color development and photographic fixing. The gray values of protein bands were analyzed and calculated using ImageJ software. GAPDH was taken as the internal control, and the relative expression of the target protein referred to the ratio of the gray value of the target band to that of the internal control band in one sample. Experiments in each group were repeated 3 times.

EdU detection

Cell culture solution was diluted with EdU by 1:500 dilution to make a 10 µM EdU stock solution. The 2× working solution of EdU in fresh medium was prepared from the 10 mM EdU stock solution, and then mixed with equal vol-

ume of adapted medium in the culture plate after warming at 37°C, followed by incubation at room temperature for 2 h and washing with PBS. The cells were fixed using 4% paraformaldehyde for 15 min, and washed 3 times with PBS containing 3% BSA after discarding the fixing solution. Then the cells were resuspended in PBS containing 0.3% Triton X-100 and incubated at room temperature for 10 min, followed by washing with PBS containing 3% BSA twice and discarding the permeabilization buffer. Then the Click-iT® EdU reaction buffer was added into each well for staining reaction. The cells in each well were incubated at room temperature in the absence of light for 30 min, and then washed 3 times with PBS containing 3% BSA. Hoechst 3334 reaction solution was subsequently added into each well. The cells in each well were incubated at room temperature in the absence of light for 10 min, and then washed 3 times, followed by observation under fluorescence microscope. The fluorescence images were visualized as red for S phase cells (proliferation cells) using the green emission and as blue for all cells using the ultraviolet emission. The proliferating cells stained by EdU and nuclei stained by Hoechst 33342 were counted from 3 randomized fields under 200-fold field of view. Cell proliferation rate = proliferation cells/total cells * 100%.

Flow cytometry

After 48 h cell transfection in groups, cell suspension was collected through trypsinization, and centrifuged, followed by washing twice with PBS buffer. Then the cells were collected by centrifugation for later use. For cell apoptosis evaluation, the re-suspended solution with about $1*10^4$ cells was taken and centrifuged. After discarding the supernatant, the cells were re-suspended in 195 μL of binding buffer. Then 5 μL Annexin V-FITC and 10 μL PI stains were added into the cell suspension, and incubated for 20 min at room temperature in the dark, followed by ice bath in the dark. The fluorescence of the cells was immediately determined by flow cytometer to evaluate the apoptosis. Experiments in each group were repeated 3 times.

For cell circle detection, the cells were fixed in 1 ml 75% ethanol precooled at -20°C and stored at 4°C overnight. Fixed cells were washed twice in precooled PBS, and were re-suspended in

500 μL PI staining solution for 30 min at 37°C in a shaking water-bath in the dark. Here, 25 μL PI stock (20×) solution and 10 μL RNase A (50×) stock solution were mixed with 500 μL staining buffer to make the PI staining solution for one sample. Cell cycle was then detected by flow cytometry at 4°C in the absence of light. Experiments in each group were repeated 3 times. Cell cycle and apoptosis analysis kits were purchased from Beyotime (Shanghai, China).

Transwell assay

Forty-eight hours after cell transfection, the cells were starved for 24 h for later use. Invasion and metastasis assays could be carried out in the same well but under different conditions. The assays used a Corning™ Transwell™ 24-well plate with 8 μm pores (USA), with 3 wells for each group. The top of the filter membrane in a Transwell insert was plated with 100 μL serum-free DMEM containing $2.5*10^5$ cells. The bottom of the lower compartment was added with 600 μL DMEM supplemented with 20% fetal bovine serum. In the migration assay, 48 h after cell transfection, the cells were fixed using 4% paraformaldehyde for 30 min. Then the well was immersed in 0.2% Triton™ X-100 (Sigma Company, St. Louis, MO, USA) for 15 min, followed by staining with 0.05% gentian violet solution for 5 min. The wells were coated with 50 μL Matrigel (Sigma Company, St. Louis, MO, USA) before the invasion assay, and fixation and staining were carried out 48 h later as above. The number of stained cells was counted underneath an inverted microscope, and 5 randomized fields of view were chosen to get an average sum of cells. Two more wells for the assays were provided for each group, and the assays were repeated 3 times, and the average value was taken as the final result.

Tumorigenicity assay in nude mice

A total of 30 BALB/c male nude mice aged 4 weeks housed in a SPF grade facility, weighing 18-25 g were purchased from Hunan SJA Laboratory Animal Co., Ltd., China. The mice were randomized into six groups, Control group, mimic NC group, miR-96-5p mimic group, oe NC group, oe PRC1 group, and miR-96-5p mimic + oe PRC1 group, with five mice in each group. After grouping, HepG2 cells were infect-
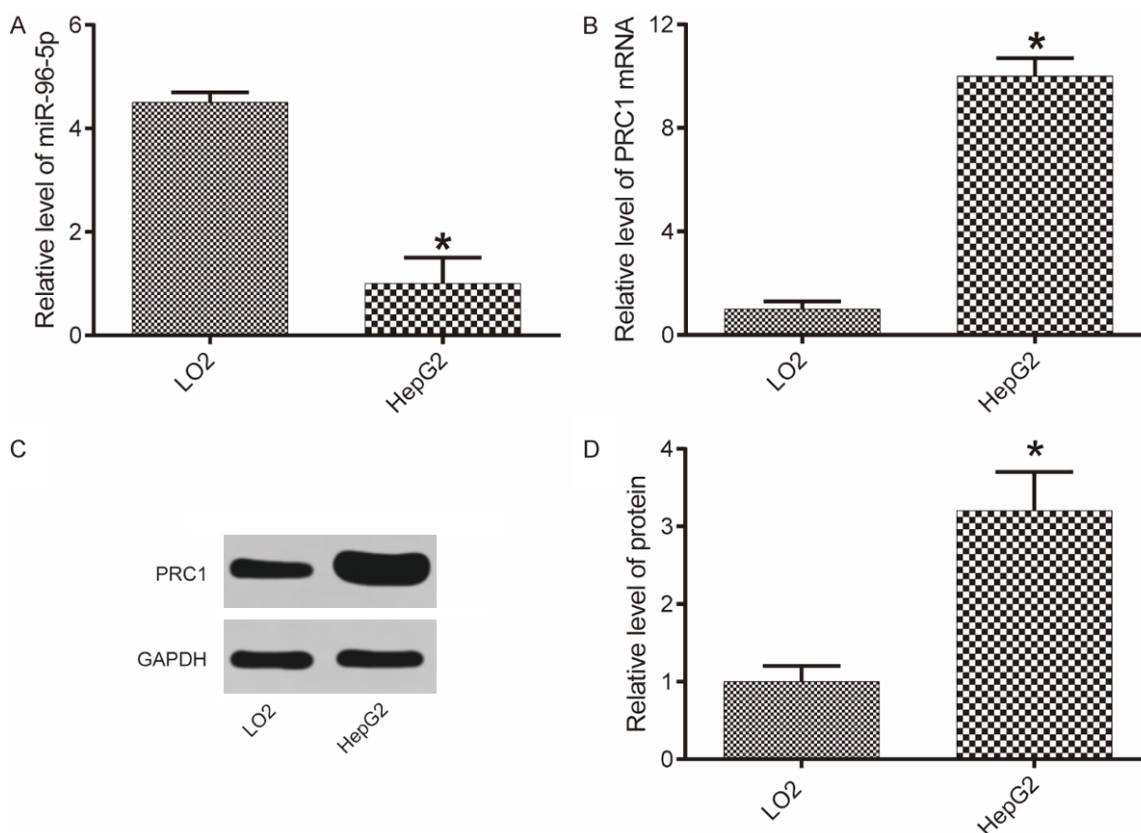
Figure 1. Expression of miR-95-5p and PRC1 in HepG2 cells. A: qRT-PCR to detect the expression level of miR-96-5p; B: qRT-PCR to detect the expression level of PRC1; C: Western blot to detect the expression level of PRC1; D: The histogram analysis. Compared with LO2 cells, *P<0.05. PRC1: protein regulator of cytokinesis 1; GAPDH: glyceraldehyde 3-phosphate dehydrogenase.

ed with lentivirus as aforementioned, and 72 h later, single-cell suspension with a concentration of $1*10^7$ cells/mL was prepared after trypsin digestion. Then 0.3 mL suspension containing about $2*10^6$ viable cells was subcutaneously injected into each nude mouse at the right flank. After cell injection, tumor volume changes were observed every five days with a Vernier caliper measuring the maximum length (a) and minimum length (b) of a tumor, and tumor volume was calculated as $(a * b^2)/2$. Thirty days later, the mice were sacrificed through massive blood loss by blood aspiration from the abdominal aorta intraperitoneally after anesthesia with intraperitoneal injection of pentobarbital sodium in the dose of 70 mg/kg, and then the tumors were removed and weighed under sterile conditions.

Statistical analysis

All the data were analyzed using the SPSS 21.0 software package (SPSS Inc., Chicago, IL, USA). The measurement data were expressed as the mean ± standard deviation. Pairwise comparisons of mean values among multiple groups were conducted using one-way analysis of variance with Fisher's least significant difference test. P value of <0.05 was considered statistically significant.

Results

Down-regulated miR-96-5p expression and up-regulated PRC1 expression in HepG2 cells

The expression of miR-96-5p and PRC1 in normal liver LO2 cells and hepatoma HepG2 cells are respectively shown in **Figure 1A**, **1B**. Compared with LO2 cells, miR-96-5P expression was significantly down-regulated and PRC1 expression was significantly up-regulated in HepG2 cells (both P<0.05). Correspondingly, **Figure 1C** shows the PRC1 expression in the two cell lines, and the results showed that the up-regulation trend of PRC1 in HepG2 cells was more obvious as compared with LO2 cells (P<0.05).
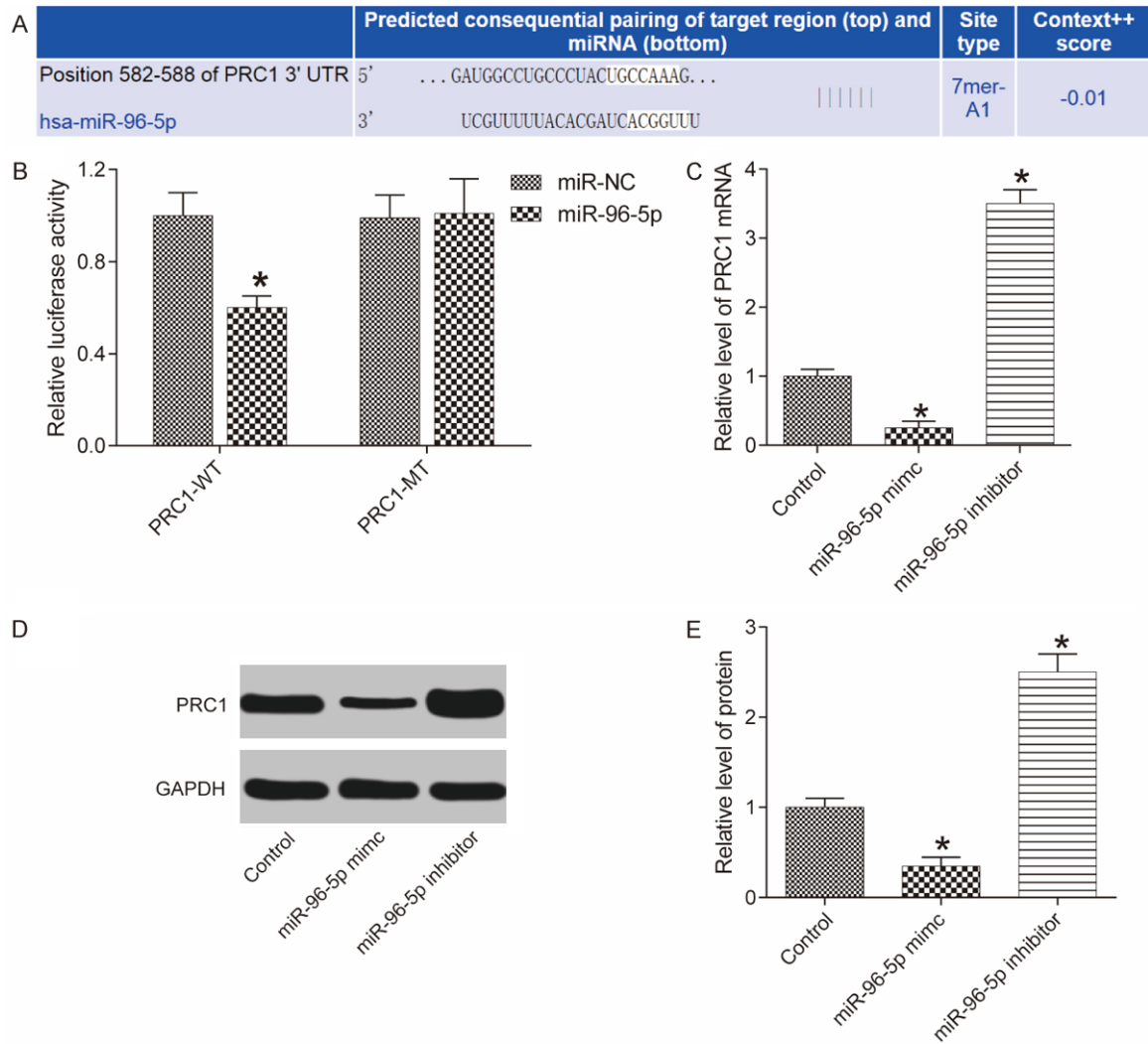
Figure 2. miR-96-5p can target PRC1 to down-regulate its expression. A: Bioinformatics website predicted and analyzed the binding site of miR-96-5p on PRC1; B: Dual-luciferase reporter gene assay verified the targeting relationship between miR-96-5p and PRC1; C: Expression level of PRC1 mRNA detected by qRT-PCR; D: PRC1 protein band detected by western blotting; E: The histogram analysis of relative protein level. Compared with control group, *P<0.05. NC: negative control; PRC1: protein regulator of cytokinesis 1; GAPDH: glyceraldehyde 3-phosphate dehydrogenase.

miR-96-5p down-regulates PRC1 expression by targeting its 3'UTR

We found a binding site between miR-96-5p and PRC1 through bioinformatics analysis (**Figure 2A**). Dual-luciferase reporter gene assay found that compared with NC group, luciferase activity intensity in co-transfection group of miR-96-5p and PRC1-WT decreased significantly (P<0.05), while co-transfection group of miR-96-5p and PRC1-MT had no obvious change in luciferase activity intensity (**Figure 2B**). In order to further explore whether miR-96-5p regulates PRC1 expression, HepG2 cells were transfected with miR-96-5p mimic and miR-96-5p inhibitor respectively. PRC1 gene and protein expressions were detected by qRT-PCR and western blot (**Figure 2C**, **2D**). Compared with Control group, PRC1 gene and protein expressions were down-regulated in miR-96-5p mimic group (both P<0.05), while the expressions were up-regulated in miR-96-5p inhibitor group (both P<0.05). These results indicate that miR-96-5p can target PRC1 to down-regulate its expression.

miR-96-5p overexpression inhibits HepG2 cell proliferation

Cell proliferation was evaluated by EdU detection (**Figure 3A**). Compared with Control group,

cell proliferation in miR-96-5p mimic group was significantly decreased (P<0.05), and that in oe PRC1 group was significantly increased (P<0.05). Compared with mimic NC group, cell proliferation in miR-96-5p mimic group was significantly decreased (P<0.05). Cell proliferation in oe PRC1 group was significantly increased as compared with oe NC group (P<0.05). Compared with miR-96-5p mimic group, cell proliferation in miR-96-5p mimic + oe PRC1 group was significantly increased (P<0.05). There was no significant difference in cell proliferation between mimic NC group and oe NC group.

Flow cytometry was conducted for cell cycle detection (**Figure 3B**). Compared with Control group, the ratio of G2/M cells in miR-96-5p mimic group was significantly higher (P<0.05), while the ratio in oe PRC1 group was significantly lower (P<0.05). The G2/M ratio in miR-96-5pmic group was significantly higher than that in mimic NC group (P<0.05). The G2/M ratio in oe PRC1 group was significantly lower than that in oe NC group (P<0.05). Compared with miR-96-5p mimic group, the G2/M ratio in miR-96-5p mimic + oe PRC1 group was significantly lower (P<0.05). There was no significant difference in the ratio between mimic NC group and oe NC group. These results indicate that PRC1 overexpression can reduce the proportion of HepG2 cells in G2/M phase and promote cell proliferation, while miR-96-5p overexpression may cause arrest at both the G1 and G2 phases of the cell cycle, thus inhibiting cell proliferation.

miR-96-5p overexpression promotes HepG2 cell apoptosis

The results of cell apoptosis through flow cytometry are shown in **Figure 4**. Compared with Control group, cell apoptosis in both miR-96-5p mimic group and miR-96-5p mimic + oe PRC1 group were significantly increased (both P<0.05). Apoptosis in miR-96-5p mimic group was significantly increased as compared with mimic NC group (P<0.05). There was no significant difference in apoptosis between oe NC group and oe PRC1 group. Cell apoptosis in miR-96-5p mimic + oe PRC1 group was significantly reduced as compared with miR-96-5p mimic group (P<0.05). Compared with oe PRC1 group, apoptosis in miR-96-5p mimic + oe PRC1 group was significantly increased (P<

0.05). There was no significant difference in cell apoptosis between mimic NC group and oe NC group.

### miR-96-5p overexpression promotes migration and invasion of HepG2 cells

Transwell assay was used to detect the migration and invasion abilities of transfected cells (**Figure 5A**, **5B**). Compared with control group, the cell migration and invasion abilities of miR-96-5p mimic group were significantly reduced (both P<0.05), while the abilities of oe PRC1 group were significantly increased (both P<0.05). Compared with mimic NC group, the abilities of miR-96-5p mimic group were significantly reduced (P<0.05). The abilities of oe PRC1 group were significantly increased as compared with oe NC group (P<0.05). Compared with miR-96-5p mimic group, the abilities of miR-96-5p mimic + oe PRC1 group were significantly increased (P<0.05). There were no significant differences in cell migration and invasion abilities between mimic NC group and oe NC group.

miR-96-5p overexpression suppresses hepatocellular carcinoma growth

The effect of miR-96-5p/PRC1 overexpression on tumor growth was detected by tumorigenicity assay in nude mice. The mice all groups were injected subcutaneously in the right axilla with HepG2 cell suspension. Food intake, activity and mental status of the mice were observed weekly. After 30-days, none of the mice died, and the tumors were removed from the sacrificed mice as shown in **Figure 6A**. Tumor tissue weight was collected and analyzed with biological statistics (**Figure 6B**). Compared with Control group, tumor tissue weight in miR-96-5p mimic group was significantly lower (P<0.05), while that in oe PRC1 group was significantly higher (P<0.05). Compared with mimic NC group, the weight in miR-96-5p mimic group was significantly lower (P<0.05). Compared with oe NC group, the tumor tissue weight in oe PRC1 group was significantly higher (P<0.05). The tumor tissue weight in miR-96-5p mimic + oe PRC1 group was significantly higher than that in miR-96-5p mimic group (P<0.05). There was no significant difference in the tumor tissue weight between mimic NC group and oe NC group.
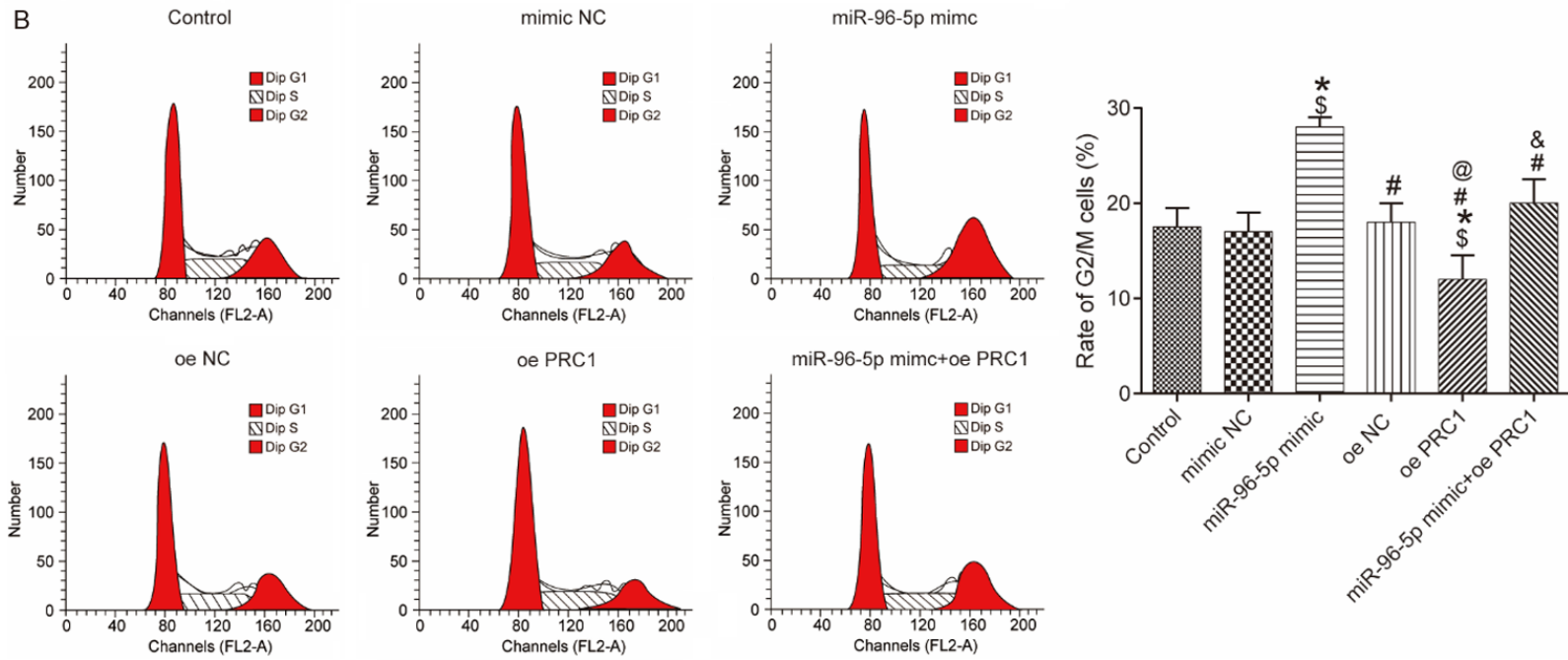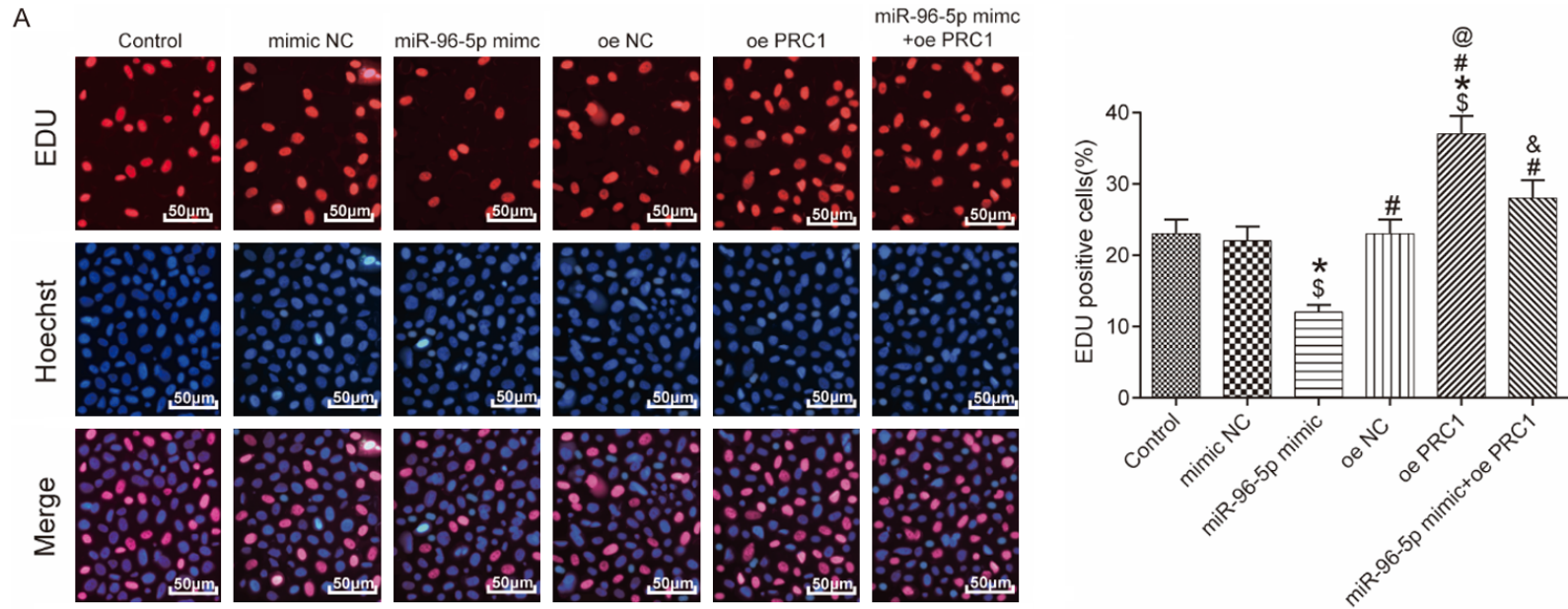
Figure 3. Proliferation of HepG2 cells. A: Cell proliferation detected by 5-ethynyl-2'-deoxyuridine and its histogram analysis; B: Cell cycle detected by flow cytometry and its histogram analysis. Compared with control group, $^\$P<0.05$; compared with mimic NC group, $^*P<0.05$; compared with miR-96-5p, $^\#P<0.05$; compared with oe NC group, $^@P<0.05$; compared with oe PRC1 group, $^\&P<0.05$. NC: negative control; PRC1: protein regulator of cytokinesis 1; EdU: 5-ethynyl-2'-deoxyuridine.
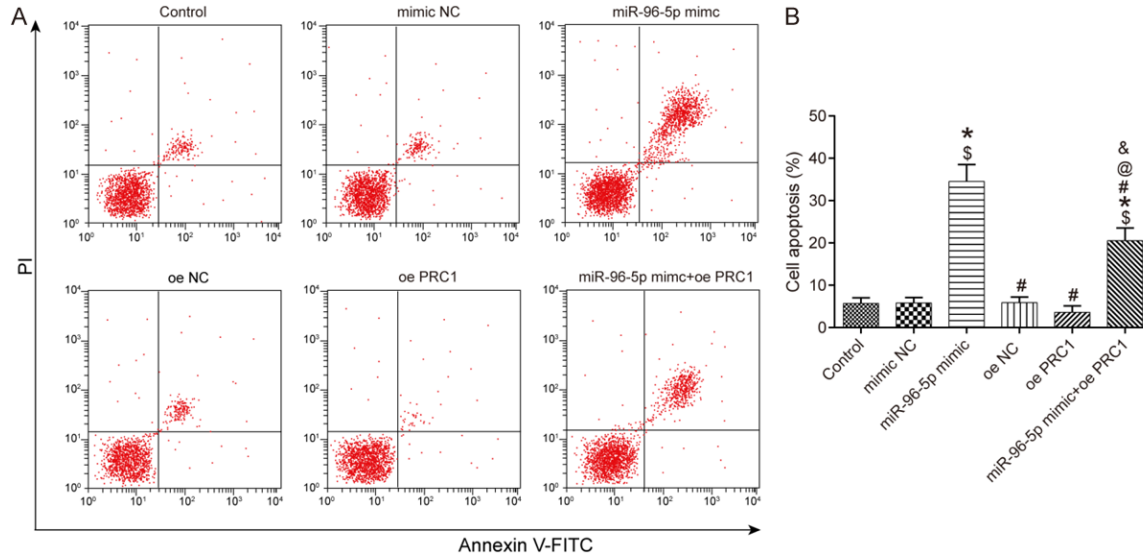
Figure 4. Apoptosis of HepG2 cells and the histogram analysis. A: Flow cytometry apoptosis chart; B: Histogram analysis chart. Compared with control group, $^\$P<0.05$; compared with mimic NC group, $^*P<0.05$; compared with miR-96-5p mimic group, $^\#P<0.05$; compared with oe NC group, $^@P<0.05$; compared with oe PRC1 group, $^\&P<0.05$. NC: negative control; PRC1: protein regulator of cytokinesis.

Tumor growth curve was drawn according to the tumor volume measured every 5 days (**Figure 6C**). The results showed that compared with Control group, the tumor tissue size in miR-96-5p mimic group was significantly smaller (P< 0.05), while that in oe PRC1 group was significantly larger (P<0.05). The tumor tissue size in miR-96-5p mimic group was significantly smaller than that in mimic NC group (P<0.05). The size in oe PRC1 group was significantly larger than that in oe NC group (P<0.05). Compared with miR-96-5p mimic group, the tumor tissue size in miR-96-5p mimic + oe PRC1 group was significantly larger (P<0.05). There was no significant difference in tumor tissue size between mimic NC group and oe NC group.

Discussion

The regulatory role of miRNAs in tumors has received wide confirmation [16]. To date, hundreds of miRNAs have been found to be closely related to the occurrence and progression of human tumors, as has miR-96-5p in this study. Research confirmed that miR-96-5p was sig-

nificantly down-regulated in early-stage hepatoma tissues in recurrent patients after radical resection of hepatocellular carcinoma [17]. MiR-96-5p plays a role in promoting survival and inhibiting platelet apoptosis during platelet storage [18], and it inhibits A549 proliferation by targeting mammalian target of rapamycin (mTOR) [19]. In this study, through detection on miR-96-5p expression in human hepatocellular carcinoma cell line HepG2 and immortalized normal human hepatic cell line LO2 using qRT-PCR, we found that miR-96-5p expression was down-regulated in hepatoma carcinoma HepG2 cells. All these results suggest that miR-96-5p may have anti-oncogene function.

To the best of our knowledge, miRNAs may contribute to various tumors in different pathological stages or be helpful to tumor therapy through targeting genes. As is known, PRC1 can be used as an indicator of malignant proliferation of tumor cells as well as of therapeutic evaluation, and it plays a crucial role in various malignant tumors such as cervical cancer, bladder cancer, prostate cancer, liver cancer
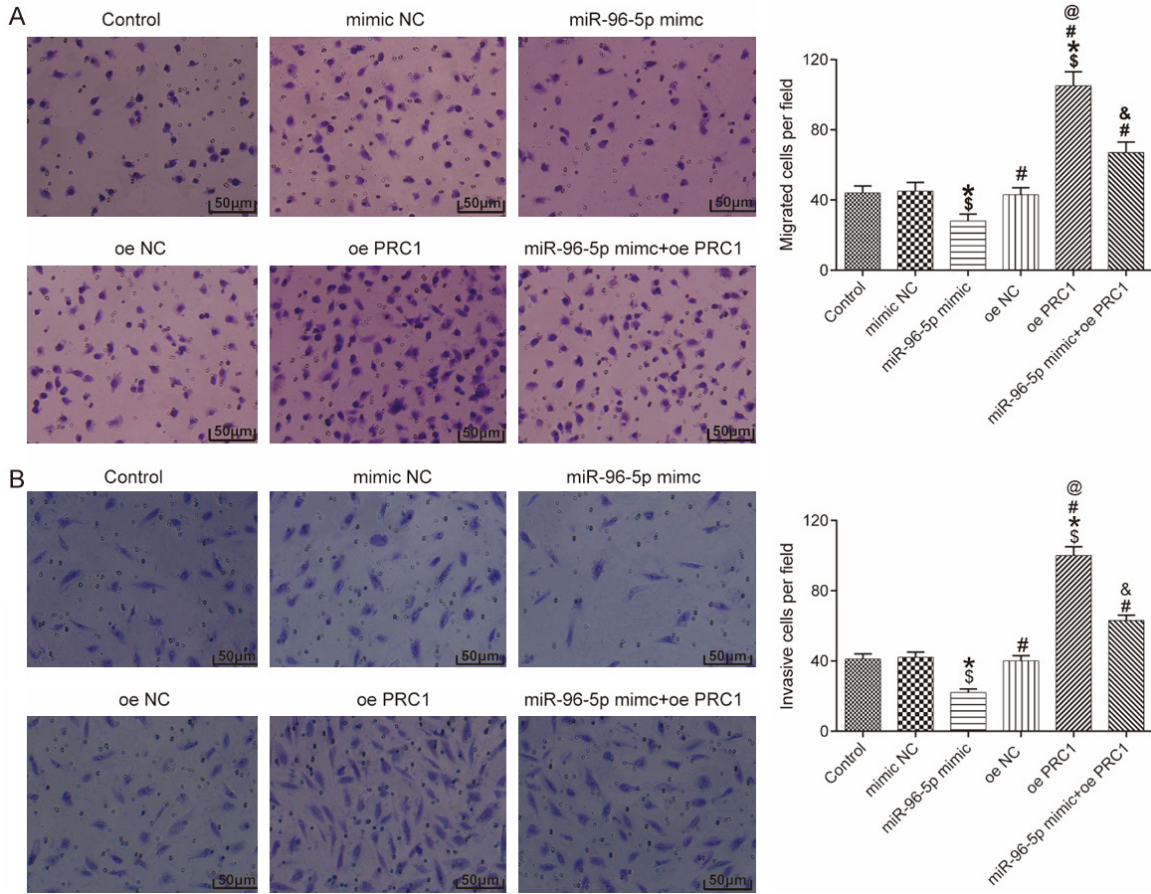
Figure 5. Migration and invasion of HepG2 cells by Transwell analysis and their histogram analyses. A: Migration of HepG2 cells by Transwell analysis and their histogram analyses; B: Invasion of HepG2 cells by Transwell analysis and their histogram analyses. Compared with control group, $P<0.05; compared with mimic NC group, *P<0.05; compared with miR-96-5p mimic group, #P<0.05; compared with oe NC group, @P<0.05; compared with oe PRC1 group, &P<0.05. NC: negative control; PRC1: protein regulator of cytokinesis 1.
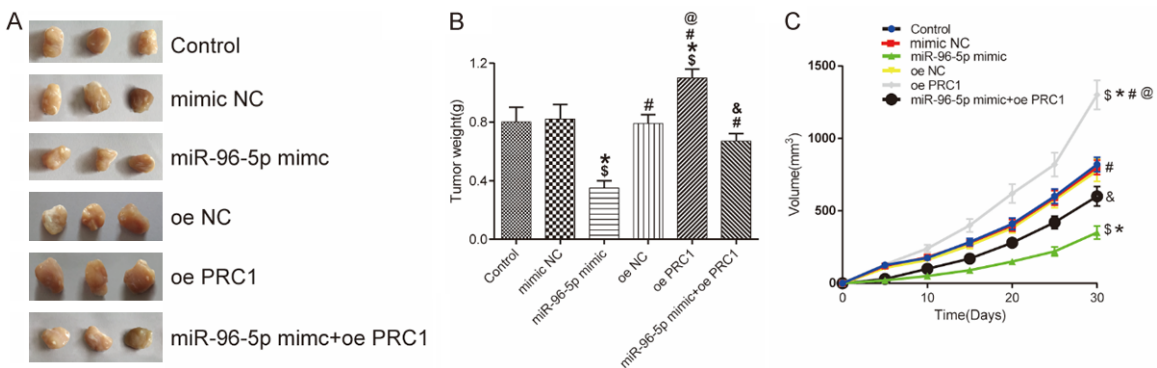
Figure 6. HepG2 cell growth of xenografted tumor. A: Contrast of tumor tissues of different groups; B: Histogram analysis of tumor weight; C: Tumor volume growth curves. Compared with control group, $P<0.05; compared with mimic NC group, *P<0.05; compared with miR-96-5p mimic group, #P<0.05; compared with oe NC group, @P<0.05; compared with oe PRC1 group, &P<0.05. NC: negative control; PRC1: protein regulator of cytokinesis 1.

and breast cancer [20-24]. Analysis of the gene expression profile with microarrays showed that the expression of PRC1 is up-regulated in almost all clinical cancers [25].

In this study we found a binding site between miR-96-5p and PRC1 through bioinformatics analysis. Dual-luciferase reporter gene assay found that miR-96-5p can target the 3'UTR of the PRC1 gene. Additionally, in the HepG2 cells, PRC1 gene and protein expression were down-regulated in miR-96-5p mimic group, while up-regulated in miR-96-5p inhibitor group as compared with Control group, indicating that miR-96-5p could target PRC1 to down-regulate its expression. MiR-96-5p may play a role in liver cancer cells by regulating the expression of PRC1.

In the phenotypic experiment, we found that overexpression of miR-96-5p can inhibit proliferation, migration and invasion of HepG2 cells and promote cell apoptosis. Inversely, overexpression of PRC1 has the opposite effects. PRC1 is a protein necessary for cell division, and is closely related to cell movement, migration and cell cycle, which may account for those results [26-28]. If aberrant cytokinesis occurs, abnormal cell division will eventually contribute to the formation of multinucleated cells and further cell mutation to carcinoma [29]. CDK1/Cyclin B1 complex controls the formation of various structures during cell mitosis and the normal progression of cell mitosis through phosphorylation of corresponding substrates, wherein PRC1 protein can be phosphorylated by CDK1/Cyclin B1 complex during cell mitosis [30]. Therefore, up-regulation of miR-96-5p can target PRC1 and inhibit its expression, thus inhibiting the proliferation, migration and invasion of HepG2 cells and promoting cell apoptosis.

In conclusion, miR-96-5p targeting the PRC1 gene inhibits proliferation and invasion of hepatoma HepG2 cells and promotes their apoptosis. However, considering that each miRNA has multiple targets, the combined action of multiple targets may account for the effect of miR-96-5p on proliferation, invasion and apoptosis of hepatoma HepG2 cells. Therefore, we will further study the role of miR-96-5p in the occurrence and progression of liver cancer from this aspect.

Disclosure of conflict of interest

None.

Address correspondence to: Xiaorong Mao, Department of Infectious Diseases, The First Hospital of Lanzhou University, No.1 Donggang West Road, Chengguan District, Lanzhou 730000, Gansu Province, China. Tel: +86-0931-8356337; Fax: +86-0931-8619797; E-mail: maoxiaoronguiy3@126.com

References

[1] Fawzy IO, Hamza MT, Hosny KA, Esmat G, El Tayebi HM and Abdelaziz AI. miR-1275: a single microRNA that targets the three IGF2-mRNA-binding proteins hindering tumor growth in hepatocellular carcinoma. FEBS Lett 2015; 589: 2257-2265.

[2] Takaoka S, Kamioka Y, Takakura K, Baba A, Shime H, Seya T and Matsuda M. Live imaging of transforming growth factor-beta activated kinase 1 activation in Lewis lung carcinoma 3LL cells implanted into syngeneic mice and treated with polyinosinic: polycytidylic acid. Cancer Sci 2016; 107: 644-652.

[3] Liu K, Wu X, Zang X, Huang Z, Lin Z, Tan W, Wu X, Hu W, Li B and Zhang L. TRAF4 regulates migration, invasion, and epithelial-mesenchymal transition via PI3K/AKT signaling in hepatocellular carcinoma. Oncol Res 2017; 25: 1329-1340.

[4] Mahringer-Kunz A, Weinmann A, Schmidtmann I, Koch S, Schotten S, Pinto Dos Santos D, Pitton MB, Dueber C, Galle PR and Kloeckner R. Validation of the SNACOR clinical scoring system after transarterial chemoembolisation in patients with hepatocellular carcinoma. BMC Cancer 2018; 18: 489.

[5] Childs A and Meyer T. Hepatocellular carcinoma: treatment. John Wiley Sons 2019; 703-714.

[6] Schulte C and Mayr M. MicroRNAs: a new understanding of platelet physiology and pathology. Thromb Haemost 2019; 119: 191.

[7] Guo W and Jing Y. Role of microRNAs in colorectal cancer: a review. World Chin J Digestol 2017; 25: 1928-1933.

[8] An X, Sarmiento C, Tan T and Zhu H. Regulation of multidrug resistance by microRNAs in anti-cancer therapy. Acta Pharm Sin B 2017; 7: 38-51.

[9] Rasko JE and Wong JJ. Nuclear microRNAs in normal hemopoiesis and cancer. J Hematol Oncol 2017; 10: 8.

[10] Hou J, Lin L, Zhou W, Wang Z, Ding G, Dong Q, Qin L, Wu X, Zheng Y, Yang Y, Tian W, Zhang Q, Wang C, Zhang Q, Zhuang SM, Zheng L, Liang A, Tao W and Cao X. Identification of miR-Nomes in human liver and hepatocellular carcinoma reveals miR-199a/b-3p as therapeutic target for hepatocellular carcinoma. Cancer Cell 2011; 19: 232-243.

[11] Leoncini PP, Bertaina A, Papaioannou D, Flotho C, Masetti R, Bresolin S, Menna G, Santoro N, Zecca M, Basso G, Nigita G, Veneziano D,

Pagotto S, D'Ovidio K, Rota R, Dorrance A, Croce CM, Niemeyer C, Locatelli F and Garzon R. MicroRNA fingerprints in juvenile myelomonocytic leukemia (JMML) identified miR-150-5p as a tumor suppressor and potential target for treatment. Oncotarget 2016; 7: 55395-55408.

[12] Jiang W, Jimenez G, Wells NJ, Hope TJ, Wahl GM, Hunter T and Fukunaga R. PRC1: a human mitotic spindle-associated CDK substrate protein required for cytokinesis. Mol Cell 1999; 2: 877-885.

[13] Wang Y, Shi F, Xing GH, Xie P, Zhao N, Yin YF, Sun SY, He J, Wang Y and Xuan SY. Protein regulator of cytokinesis PRC1 confers chemoresistance and predicts an unfavorable postoperative survival of hepatocellular carcinoma patients. J Cancer 2017; 8: 801-808.

[14] Dolbniak M, Kimmel M and Smieja J. Modeling epigenetic regulation of PRC1 protein accumulation in the cell cycle. Biol Direct 2015; 10: 62.

[15] Loubiere V, Delest A, Thomas A, Bonev B, Schuettengruber B, Sati S, Martinez AM and Cavalli G. Coordinate redeployment of PRC1 proteins suppresses tumor formation during drosophila development. Nat Genet 2016; 48: 1436-1442.

[16] Matamala N, Vargas MT, Gonzalez-Campora R, Minambres R, Arias JI, Menendez P, Andres-Leon E, Gomez-Lopez G, Yanowsky K, Calvete-Candenas J, Inglada-Perez L, Martinez-Delgado B and Benitez J. Tumor microRNA expression profiling identifies circulating microRNAs for early breast cancer detection. Clin Chem 2015; 61: 1098-1106.

[17] Lai QB, Jin HS, Jian ZX, University SM and Hospital GG. Expression and clinical significance of miR-96-5p in primary hepatocellular carcinoma at early recurrence after radical surgery. J Pract Med 2014.

[18] Hengshi XU, Yang Y and Cui H. Study of the mechanism of miR-96-5p in anti-apoptosis induced by storage in platelet. Chin Med Herald 2018.

[19] Liu D, Peng J, Jun LI and Zheng S. Upregulation of miR-96-5p inhibits the proliferation of lung adenocarcinoma cell A549. J Pract Med 2017.

[20] Wu F, Shi X, Zhang R, Tian Y, Wang X, Wei C, Li D, Li X, Kong X, Liu Y, Guo W, Guo Y and Zhou H. Regulation of proliferation and cell cycle by protein regulator of cytokinesis 1 in oral squamous cell carcinoma. Cell Death Dis 2018; 9: 564.

[21] Zhan P, Xi GM, Liu HB, Liu YF, Xu WJ, Zhu Q, Zhou ZJ, Miao YY, Wang XX, Jin JJ, Lv TF and Song Y. Protein regulator of cytokinesis-1 expression: prognostic value in lung squamous cell carcinoma patients. J Thorac Dis 2017; 9: 2054-2060.

[22] Liu X, Li Y, Meng L, Liu XY, Peng A, Chen Y, Liu C, Chen H, Sun S, Miao X, Zhang Y, Zheng L and Huang K. Reducing protein regulator of cytokinesis 1 as a prospective therapy for hepatocellular carcinoma. Cell Death Dis 2018; 9: 534.

[23] Li J, Dallmayer M, Kirchner T, Musa J and Grunewald TGP. PRC1: linking cytokinesis, chromosomal instability, and cancer evolution. Trends Cancer 2018; 4: 59-73.

[24] Johnson CA, Wright CE and Ghashghaei HT. Regulation of cytokinesis during corticogenesis: focus on the midbody. FEBS Lett 2017; 591: 4009-4026.

[25] Yu F, Zhou C, Zeng H, Liu Y and Li S. BMI1 activates WNT signaling in colon cancer by negatively regulating the WNT antagonist IDAX. Biochem Biophys Res Commun 2018; 496: 468-474.

[26] Zhang B, Shi X, Xu G, Kang W, Zhang W, Zhang S, Cao Y, Qian L, Zhan P, Yan H, To KF, Wang L and Zou X. Elevated PRC1 in gastric carcinoma exerts oncogenic function and is targeted by piperlongumine in a p53-dependent manner. J Cell Mol Med 2017; 21: 1329-1341.

[27] Mollinari C, Kleman JP, Saoudi Y, Jablonski SA, Perard J, Yen TJ and Margolis RL. Ablation of PRC1 by small interfering RNA demonstrates that cytokinetic abscission requires a central spindle bundle in mammalian cells, whereas completion of furrowing does not. Mol Biol Cell 2005; 16: 1043-1055.

[28] Li C, Lin M and Liu J. Identification of PRC1 as the p53 target gene uncovers a novel function of p53 in the regulation of cytokinesis. Oncogene 2004; 23: 9336-9347.

[29] Straight AF and Field CM. Microtubules, membranes and cytokinesis. Curr Biol 2000; 10: R760-770.

[30] Kurasawa Y, Earnshaw WC, Mochizuki Y, Dohmae N and Todokoro K. Essential roles of KIF4 and its binding partner PRC1 in organized central spindle midzone formation. Embo J 2004; 23: 3237-3248.